A Precise Seasonal Air-Sea Gas Exchange Rate from Observing the Ocean Breath Noble Gases

Rachel H. R. Stanley*[1], William J. Jenkins[2], Dempsey E. Lott III[2], & Scott C. Doney[2]

[1] *Department of Geosciences, Princeton University, Guyot Hall, Princeton, NJ 08544, USA*

[2]*Department of Marine Chemistry and Geochemistry, Woods Hole Oceanographic Institution, 266 Woods Hole Road, Woods Hole, MA 02453, USA*

* corresponding author: rstanley@princeton.edu

Contact Information for authors:

Rachel H.R. Stanley*, rstanley@princeton.edu, Tel: 609-258-2756. Fax: 609-258-0796

William J. Jenkins, wjenkins@whoi.edu, Tel: 508-289-2554. Fax: 508-457-2193

Dempsey E Lott, III, dlott@whoi.edu, Tel: 508-289-2925. Fax: 508-457-2193

Scott C. Doney, doney@whoi.edu, Tel: 508-289-3776. Fax: 508-457-2193

Air-sea gas exchange is a crucial component of the biogeochemical cycles of many climatically relevant gases including CO_2, O_2, CH_4, and N_2O. Accurate representation of air-sea gas exchange in climate models is clearly important. Several wind-speed dependent parameterizations of air-sea gas exchange exist [1-5], but such parameterizations have large uncertainties, are based on either very short (hours[3] to days[2,4]) or long (decadal[1,5]) time-scales, and do not explicitly include bubble fluxes. We used a two year time-series of observations of five noble gases (He, Ne, Ar, Kr, and Xe) at the Bermuda Atlantic Time-series Study (BATS) site in tandem with a one-dimensional upper-ocean model to develop an improved parameterization for air-sea gas exchange. Based on seasonal time-scale data, the parameterization has much tighter constraints than previous methods: ± 15% for diffusive gas exchange and ±30% for bubble fluxes. The magnitude of diffusive gas exchange is 90% of that of Wanninkhof [1], the most commonly used parameterization, and thus most previous estimates of air-sea gas exchange may have overestimated fluxes. Additionally, we found that bubble-mediated exchange, which is commonly neglected, is significant even for soluble gases and therefore needs to be explicitly included in a range of marine biogeochemical calculations that incorporate air-sea gas fluxes. The parameters presented here are valid for regions that have similar wind conditions to the Sargasso Sea (between 0 and 15 m s^{-1}) and that are similarly oligotrophic.

The noble gases are biologically and chemically inert, making them ideal physical tracers. Additionally, the five stable noble gases differ in solubility by a factor of ten and in molecular diffusivity by a factor of five. This large range in physiochemical characteristics makes the gases respond differently to physical forcing. Helium and neon, the least soluble gases, are sensitive to both diffusive gas exchange and to air injection (bubble) processes. Krypton and xenon, which are more soluble and

have a strong temperature dependence to solubility, respond primarily to thermal forcing and diffusive gas exchange. Argon has intermediate behaviour and is useful as an abiotic analogue for oxygen. In the subtropical Atlantic, surface water temperature changes by as much as 10˚C on a seasonal basis, changing the solubility of gases significantly. Also, the mean wind speed changes from ~ 5.1 m s^{-1} in the summer to 7.3 m s^{-1} in the winter. The degree to which the water column does not maintain perfect equilibrium with the atmosphere is a measure of the gas exchange rate, and thus measurements of the seasonal cycle of all the noble gases concurrently allow separation and quantification of air-sea gas exchange processes.

A two-year time-series of the five noble gases (Fig. 1a) measured at the BATS site in the Sargasso Sea reveals that the gases fall into two distinct groups. Helium and neon, relatively insoluble, are always a few percent supersaturated in the upper ocean because of bubble processes and do not show seasonal structure. The He and Ne saturation anomaly data are noisy due to bubbles inadvertently trapped during sample collection. (Saturation anomaly refers to the percent departure from equilibrium: $(C_w/C_{eq}-1)x100$, where C_w is the concentration of the gas in the seawater and C_{eq} is the concentration of the gas at equilibrium.) Argon, krypton, and xenon form the second group. These gases show maximal saturation anomalies in the summer, especially below the mixed layer. The gases are less soluble in warmer water and thus in the summer become supersaturated. This drives a diffusive gas exchange flux out of the water. Because Xe has the strongest temperature dependence on solubility, the supersaturation of Xe is the largest.

In the surface mixed layer, the gases also act as two distinct groups (Fig. 2). Helium and neon have little seasonal variation and are always supersaturated. Argon, krypton, and xenon in contrast are supersaturated in the summertime and at saturation or undersaturated in the winter-time. The relative magnitudes of the supersaturation of

these gases correlate with the temperature dependency of solubility: Xe has the largest summer supersaturation and Ar the smallest. Uncertainties in our knowledge of the solubilities of the noble gases[6-10] could cause these saturation anomalies to systematically shift to higher or lower values.

In order to use the noble gas data to improve parameterizations of air-sea gas exchange, we use a one-dimensional numerical model[11-13] to explore the sensitivity of air-sea gas exchange parameters to noble gas measurements. The 1-D model is forced with high-frequency, synoptic atmospheric physical forcing[14] using six hourly NCEP reanalysis heat fluxes[15] and 12 hourly QuikSCAT winds. Physical parameters in the model are tuned to match the temperature and salinity data obtained at BATS.

The diffusive gas exchange flux is modelled according to Wanninkhof[1], where the gas transfer velocity varies with the square of the 10 m wind speed, but with a scaling parameter to adjust the magnitude of the flux. Specifically, the diffusive gas exchange flux, F_{GE} in mol m^{-2} s^{-1}, is modelled according to the equation

$$F_{GE} = \gamma_G \cdot 8.6 \times 10^{-7} \left(\frac{Sc}{660} \right)^{-0.5} u_{10}{}^2 \left(C_{i,eq} - C_{i,w} \right) \qquad (1)$$

where γ_G is a tunable model parameter that controls the magnitude of diffusive gas exchange, *Sc* is the Schmidt number, u_{10} is the wind speed in m s^{-1} at a height of 10 m above the sea surface, $C_{i,eq}$ is the concentration of the gas i at equilibrium, and $C_{i,w}$ is the concentration of the gas *i* in the water. In this study, the noble gases were used to constrain γ_G to equal 0.90 ± 0.13.

The air injection flux is separated into two components[12,16,17]. The first component comprises completely trapped bubbles - bubbles that dissolve completely and thus inject gases with atmospheric abundances. The flux due to completely trapped bubbles, Fc, is parameterized using the whitecap coverage parameterization of Monohan

and Torgersen[18] and the air entrainment velocity of Keeling[19]. The flux, in mol m^{-2} s^{-1}, is parameterized as

$$F_C = A_c (u_{10} - 2.27)^3 \frac{P_{i,a}}{RT} \qquad (2)$$

where A_c is a tunable model parameter which includes constants from the air entrainment velocity and whitecap formulations, $P_{i,a}$ is the partial pressure of gas *i* in the atmosphere (Pa), *R* is the gas constant (8.31 J mol^{-1} K^{-1}), and *T* is the temperature (K). In this study, noble gases were used to constrain A_c to equal 9.1 (±2.2) x 10^{-11}.

The second component comprises bubbles that are only partially dissolved. These bubbles, which are often larger, are injected and then rise to the surface and thus the injected gases are fractionated according to their permeation rate[13,19]. The partially trapped bubble flux therefore depends on the solubility and diffusivity of the gas, as well as the depth to which the bubble is injected. The flux is given in mol m^{-2} s^{-1} by

$$F_P = A_p \cdot (u_{10} - 2.27)^3 \alpha_i D_i^{2/3} \frac{\left(P_{i,b} - P_{i,w}\right)}{RT} \qquad (3)$$

where A_p is a tunable model parameter controlling the magnitude of the diffusive gas exchange flux, α is the Bunsen solubility coefficient of gas *i*, *D* is the diffusivity coefficient of gas *i* (m^2 s^{-1}), $P_{i,b}$ is the pressure of gas *i* in the bubble and $P_{i,w}$ is the partial pressure of gas *i* in the water. $P_{i,b}$ is approximated by $P_{i,b} = X_i\left(P_{\text{atm}} + \rho g(0.15 \cdot u_{10} - 0.55\right)$ where X_i is the mole fraction of gas *i* in dry air, P_{atm} is the atmospheric pressure of dry air (Pa), ρ is the density of water (kg m^{-3}), and *g* is the gravitational acceleration (9.81 m s^{-1}). For an explanation of the rationale behind this parameterization, see Stanley et al[13]. In this study, noble gases were used to constrain A_p to equal (1.0 ± 2.8) x 10^{-3}. Note that even though the uncertainty on A_p is large, since the partially trapped bubble flux is only a small contribution (1 to 5% of the total air injection flux), the uncertainty on the total air injection flux is only ± 30%.

We embedded the 1D model in a nonlinear optimization scheme. A cost function, based on model-data differences of noble gas surface saturation anomalies and subsurface concentrations, is used to determine the values for adjustable parameters controlling the magnitude of these three types of gas exchange fluxes: diffusive gas exchange magnitude, completely trapped bubbles, and partially trapped bubbles. These parameters can now be applied to calculate the flux of any gas of interest, e.g. CO_2, O_2, N_2O, etc. Figure 1 illustrates the very good agreement between the model and the data. The largest discrepancy between model and data occurs in July and August 2004, due to the passage of an eddy. Our results are not significantly affected by the inclusion or omission of data from these months. Thus, the noble gas data provides a method for determining these air-sea gas exchange parameters with much smaller uncertainties than previous methods and for constraining these parameters on seasonal time-scales, a unique and relevant time-scale.

The diffusive gas exchange rate is constrained to an uncertainty of ±15%. The magnitude of the diffusive gas exchange parameter is 0.90 ± 0.14, implying that the commonly used Wanninkhof relationship may overestimate gas exchange fluxes by 10%. If the solubilities of Kr and Xe were better determined, the diffusive gas exchange rate could be constrained to ± 5% using the data presented here. Note that this estimate of diffusive gas exchange parameter is determined using QuikSCAT winds. If a different wind-product is used (NCEP reanalysis winds for example) then adjustment may need to be made. This new estimate of the gas exchange parameter is consistent with recent studies using independent methods[4,5] but those had lower gas exchange parameters and did not explicitly include air injection processes. We determined the magnitude of the air injection processes to ±30%, limited by the accuracy of the He and Ne measurements. These estimates are valid over the range of wind speeds observed at Bermuda (0-15 m s^{-1}) and for waters low in surfactants (i.e. oligotrophic waters)[20].

The model can also be used to examine the relative contribution of diffusive gas exchange fluxes versus air injection fluxes for the different gases (Fig. 3). For He, the least soluble gas studied, the air injection flux is balanced by the diffusive gas exchange flux. For Ar, which is of interest since it responds physically in a similar manner as O_2, the air injection flux in the winter (when wind speeds are greater) is also nearly balanced by the diffusive gas exchange flux. Seasonal cycles of oxygen are used to constrain new production both from data[21] and from models[22,23]. This study shows that models of seasonal oxygen cycling that do not explicitly include bubble fluxes will not accurately constrain net community production since the bubble flux is approximately the same size as the diffusive gas exchange flux.

Surprisingly, even for Xe, the most soluble of the noble gases, the air injection flux in the wintertime is significant, being approximately equal to the diffusive gas exchange flux. Thus this work shows that bubble fluxes are more important than previous believed and should be explicitly included, especially for gases with solubilities equal to or less than that of Xe, such as O_2 and N_2. Moreover, the lower gas exchange rate and the air injection flux, as determined here, when applied to the surface water CO_2 climatology[24], will give lower seasonal fluxes and a smaller net CO_2 uptake by the ocean.

In summary, the five noble gases have a wide range in physicochemical characteristics and are biologically and chemically inert. This makes simultaneous measurements of all five noble gases a powerful tool for diagnosing air-sea exchange on seasonal time-scales. The parameterizations determined through the noble gases can now be applied to calculate more accurate and precise fluxes of CO_2, O_2 and other gases of climatic importance.

Methods

Samples for noble gases were collected at the BATS site (31.7 °N, 64.2°W) every month directly from Niskin bottles by gravity feeding through tygon tubing into valved stainless steel sample cylinders (90 cc volume). We extracted gases from the sample cylinders into aluminosilicate glass bulbs at an on-shore laboratory within 24 hours of sampling[25]. The alimunosilicate bulbs were attached to a dual mass spectrometric system and analyzed for He, Ne, Ar, Kr, and Xe. The noble gases in the water sample were chemically purified by sequential drawing through a two-stage water vapour cryotrap to remove water vapour, through a Pd catalyst to remove methane, and through Ti-Zr-Fe getters to remove active gases such as O_2, N_2, and H_2. The noble gases were then drawn onto two cryogenic traps[26]: a stainless steel cryogenic trap for Ne, Ar, Kr and Xe and an activated charcoal cryogenic trap for He. The cryogenic traps were selectively warmed, and the noble gases were sequentially released into a statically operated, Hiden Quadrupole Mass Spectrometer (QMS) for measurement by peak height manometry. Standardization of the system was accomplished using precisely known aliquots of atmospheric gases. Corrections are made for small nonlinearity and matrix effects. Reproducibility from duplicate water samples is better than 0.3% for Ar, Kr, and Xe and approximately 1% for He and Ne.

References

1. Wanninkhof, R. Relationship between wind speed and gas exchange over the ocean. *Journal of Geophysical Research* **97**, 7373-7382 (1992).
2. Nightingale, P. D. et al. In situ evaluation of air-sea gas exchange parameterizations using novel conservative and volatile tracers. *Global Biogeochemical Cycles* **14**, 373-387 (2000).
3. Wanninkhof, R. & McGillis, W. R. A cubic relationship between air-sea CO_2 exchange and wind speed. *Geophysical Research Letters* **26**, 1889-1892 (1999).

4. Ho, D. T. et al. Measurements of air-sea gas exchange at high wind speeds in the Southern Ocean: Implications for global parameterizations. *Geophysical Research Letters* **33** (2006).
5. Sweeney, C. et al. Constraining global air-sea gas exchange for CO2 with recent bomb C-14 measurements. *Global Biogeochemical Cycles* **21** (2007).
6. Weiss, R. F. The solubility of nitrogen, oxygen and argon in water and seawater. *Deep-Sea Research* **17**, 721-735 (1970).
7. Weiss, R. F. Solubility of helium and neon in water and seawater. *Journal of Chemical Engineering Data* **16**, 235-241 (1971).
8. Weiss, R. F. & Kyser, T. K. Solubility of krypton in water and seawater. *Journal of Chemical Engineering Data* **23**, 69-72 (1978).
9. Hamme, R. C. & Emerson, S. The solubility of neon, nitrogen and argon in distilled water and seawater. *Deep Sea Research I* **51**, 1517-1528 (2004).
10. Wood, D. & Caputi, R. 14. (U.S. Naval Radiological Defense Laboratory, San Francisco, CA, 1966).
11. Price, J. F., Weller, R. A. & Pinkel, R. Diurnal cycling - observations and models of the upper ocean response to diurnal heating, cooling, and wind mixing. *Journal of Geophysical Research-Oceans* **91**, 8411-8427 (1986).
12. Spitzer, W. S. & Jenkins, W. J. Rates of vertical mixing, gas-exchange and new production - estimates from seasonal gas cycles in the upper ocean near Bermuda. *Journal of Marine Research* **47**, 169-196 (1989).
13. Stanley, R. H. R., Jenkins, W. J. & Doney, S. C. Quantifying seasonal air-sea gas exchange processes using noble gas time-series: A design experiment. *Journal of Marine Research* **64**, 267-295 (2006).
14. Doney, S. C. A synoptic atmospheric surface forcing data set and physical upper ocean model for the U.S. JGOFS Bermuda Atlantic Time-series Study Site. *Journal of Geophysical Research* **101**, 25615-25634 (1996).
15. Kalnay, E. et al. The NCEP/NCAR 40-year reanalysis project. *Bulletin of the American Meteorological Society* **77**, 437-471 (1996).
16. Hamme, R. C. & Emerson, S. R. Constraining bubble dynamics and mixing with dissolved gases: Implications for productivity measurements by oxygen mass balance. *Journal of Marine Research* **64**, 73-95 (2006).
17. Fuchs, G., Roether, W. & Schlosser, P. Excess 3He in the ocean surface layer. *Journal of Geophysical Research* **92**, 6559-6568 (1987).
18. Monahan, E. C. & Torgersen, T. in *Air-Water Mass Transfer, Second International Symposium on Gas Transfer at Water Surfaces* 608-617 (ASCE, NY, 1990).
19. Keeling, R. F. On the role of large bubbles in air-sea gas-exchange and supersaturation in the ocean. *Journal of Marine Research* **51**, 237-271 (1993).
20. Frew, N. M. et al. Air-sea gas transfer: Its dependence on wind stress, small-scale roughness, and surface films. *Journal of Geophysical Research-Oceans* **109** (2004).
21. Jenkins, W. J. & Goldman, J. C. Seasonal oxygen cycling and primary production in the Sargasso Sea. *Journal of Marine Research* **43**, 465-491 (1985).
22. Najjar, R. G. & Keeling, R. F. Mean annual cycle of the air-sea oxygen flux: A global view. *Global Biogeochemical Cycles* **14**, 573-584 (2000).

23. Jin, X., Najjar, R. G., Louanchi, F. & Doney, S. C. A modeling study of the seasonal oxygen budget of the global ocean. *Journal of Geophysical Research-Oceans* **112** (2007).
24. Takahashi, T. et al. Global sea-air CO2 flux based on climatological surface ocean pCO(2), and seasonal biological and temperature effects. *Deep-Sea Research Part Ii-Topical Studies in Oceanography* **49**, 1601-1622 (2002).
25. Lott, D. E. & Jenkins, W. J. Advances in analysis and shipboard processing of tritium and helium samples. *International WOCE Newsletter* **30**, 27-30 (1998).
26. Lott, D. E. Improvements in noble gas separation methodology: a nude cryogenic trap. *Geochemistry, Geophysics, Geosystems* **2**, 10.129/2001GC000202 (2001).

Acknowledgements

We thank Michael Lomas, Rod Johnson, all other scientists associated with the BATS program, and the captain and crew of the *R/V Weatherbird II* for assistance in collecting samples. We are grateful to funding from the National Science Foundation Chemical Oceanography program (OCE-0221247).

Figure Legends

Figure 1. Saturation anomalies of the five noble gases in the upper 160m of the Sargasso Sea. Saturation anomalies were (a) measured in a two year time-series at the BATS site and (b) modelled using a one-dimensional numerical model. Because the noble gases track physical processes and have a factor of ten difference in solubility, measurements of all five noble gases provide tight constraints on air-sea gas exchange rates. Helium and neon, which are relatively insoluble, are always a few percent supersaturated because of air injection processes. Argon, krypton, and xenon, which have a strong thermal dependence to solubility, are at a maximum in the summer as the water warms. The white dots correspond to sample depths, and the thin white line denotes the mixed layer depth.

Figure 2. Saturation anomalies in the surface ocean (a) for helium and neon and (b) for argon, krypton, and xenon. In both the model and the data, He and Ne are always a few percent supersaturated and show little seasonal variation. In contrast, Ar, Kr, and Xe show a distinct seasonal pattern with Xe being the most supersaturated in the summer. Circles represent the average of multiple measurements within the mixed layer, with the error bars reflecting the standard error of the mean. Solid lines denote model results.

Figure 3. Diffusive gas exchange and air injection fluxes for three of the noble gases. Diffusive gas exchange fluxes (red), completely trapped bubble fluxes (blue), and the partially trapped bubble fluxes (green) for (a) He, (b) Ar, and (c) Xe as calculated by the model. Positive (negative) fluxes represent fluxes of gas into (out of) the ocean. The bubble fluxes are largest in the winter-time since the winds are strongest then. Bubble fluxes are significant in the winter for all the gases, even for the more soluble gases such as Ar (and thus O_2), and Xe.

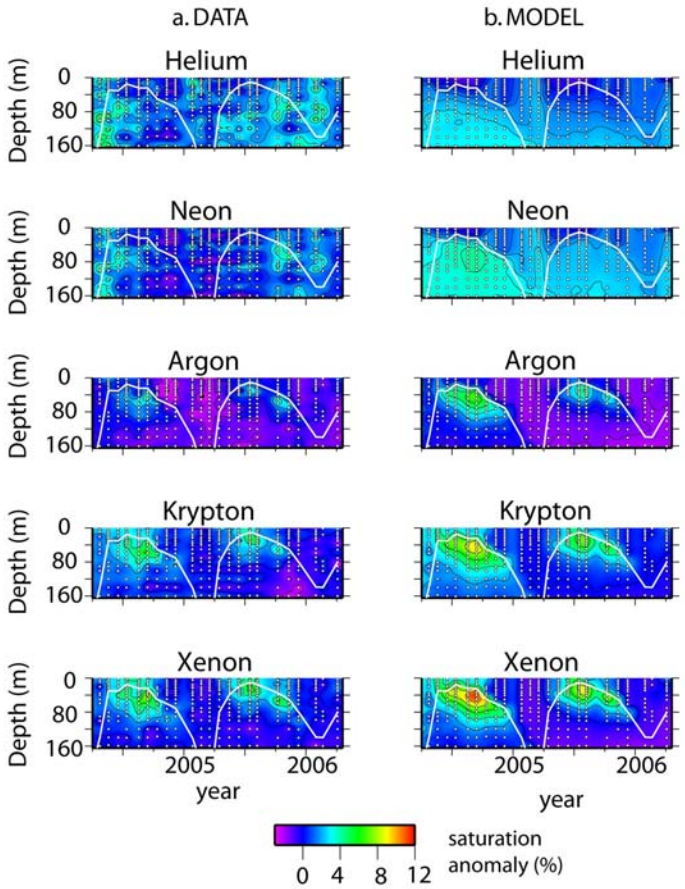

Figure 1. Saturation anomalies of the five noble gases in the upper 160 m of the Sargasso Sea. Saturation anomalies were (a) measured in a two year time-series at the BATS site and (b) modelled using a one-dimensional numerical model. Because the noble gases track physical processes and have a factor of ten difference in solubility, measurements of all five noble gases provide tight constraints on air-sea gas exchange rates. Helium and neon, which are relatively insoluble, are always a few percent super-saturated because of air injection processes. Argon, krypton, and xenon, which have a strong thermal dependence to solubility, are at a maximum in the summer as the water warms. The white dots correspond to sample depths, and the thin white line denotes the mixed layer depth.

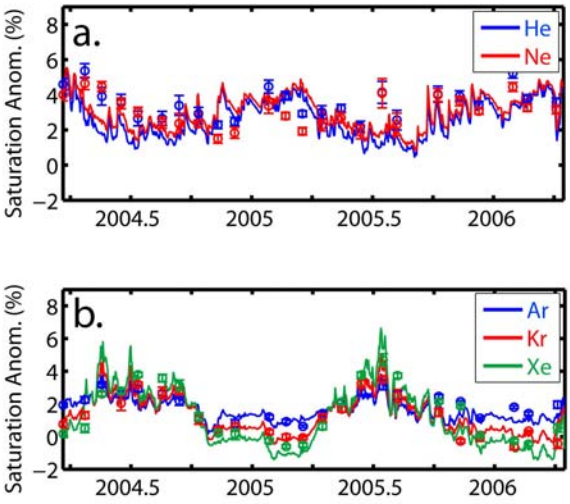

Figure 2. Saturation anomalies in the surface ocean (a) for helium and neon and (b) for argon, krypton, and xenon. In both the model and the data, He and Ne are always a few percent supersaturated and show little seasonal variation. In contrast, Ar, Kr, and Xe show a distinct seasonal pattern with Xe being the most supersaturated in the summer. Circles represent the average of multiple measurements within the mixed layer, with the error bars reflecting the standard error of the mean. Solid lines denote model results.

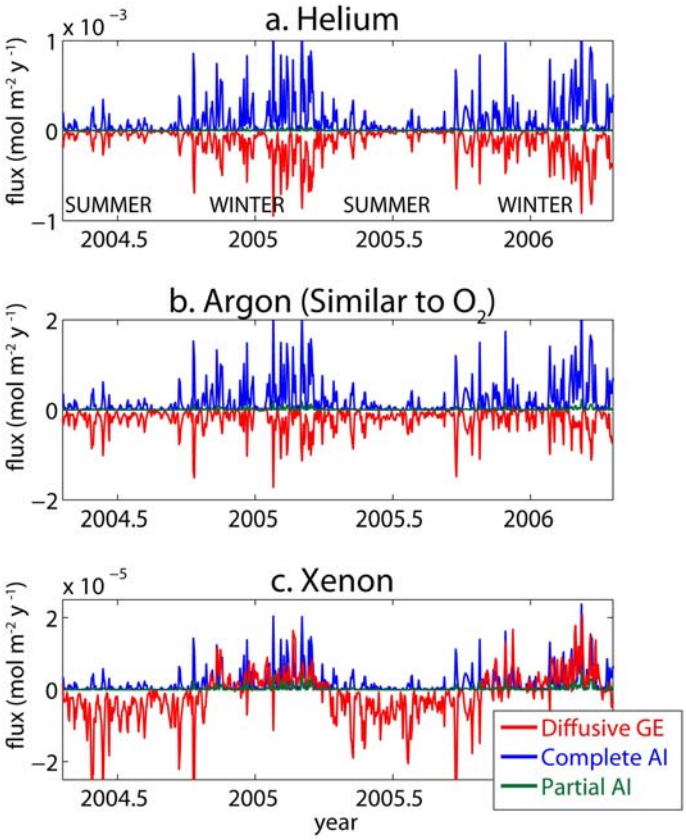

Figure 3. Diffusive gas exchange and air injection fluxes for three of the noble gases. Diffusive gas exchange fluxes (red), completely trapped bubble fluxes (blue), and partially trapped bubble fluxes (green) for (a) He, (b) Ar, and (c) Xe as calculated by the model. Positive (negative) fluxes represent fluxes of gas into (out of) the ocean. The bubble fluxes are largest in the winter-time since the winds are strongest then. Bubble fluxes are significant in the winter for all the gases, even for the more soluble gases such as Ar (and thus O_2), and Xe.